Exploring the sustainable production of ammonia by recycling N and H in biological residues: evolution of fuel-N during glutamic acid gasification

Gil-Lalaguna, N., [1] Afailal, Z.,[1] Aznar, M.,[3] Fonts, I. [1,2,*]

*Corresponding author: isabelfo@unizar.es

[1]*Thermochemical Processes Group, Aragon Institute for Engineering Research (I3A), Chemical and Environmental Engineering Department, University of Zaragoza, C/ Mariano Esquillor s/n, 50.018 Zaragoza, Spain*

[2]*Chemical and Environmental Department, Centro Universitario de la Defensa, Academia General Militar, Ctra. Huesca s/n, 50.090 Zaragoza, Spain*

[3]*Department of Mechanical Engineering, University of Zaragoza, María de Luna s/n, 50018 Zaragoza, Spain*

Amount of words = 11528

ABSTRACT

In this work, the recycling of nitrogen and hydrogen from nitrogen rich (N-rich) biological residues via autothermal gasification has been proposed as a process suitable for the sustainable production of ammonia (NH_3). Two N-rich biological residues, sewage sludge (SS) and meat and bone meal (MBM), were analyzed and glutamic acid (GLU) was selected as the model compound of the protein-fuel-N in these residues. GLU gasification experiments were carried out in order to study the effect of temperature (800-900 ºC) and steam-to-carbon ratio (0.5-1.0 $g \cdot g^{-1}$) on the conversion of fuel-N into the most typical N-containing gasification products: NH_3, molecular nitrogen (N_2), hydrogen cyanide (HCN), nitrogen monoxide (NO), tar-N and char-N. SS and MBM were also

gasified under selected operating conditions with the main aim of assessing the NH_3 production. The most abundant N-containing compounds obtained in the gasification of GLU were NH_3 (35-51% over fuel-N) and N_2 (45-63% over fuel-N). The highest conversion of fuel-N to NH_3-N in the GLU gasification experiments (51%) was obtained at the lowest temperature (800 ºC) and the lowest S/C ratio (0.5 $g \cdot g^{-1}$) studied. The increase in the temperature caused a decrease in the yield of NH_3, as a consequence of its decomposition into N_2. A similar fuel-N distribution was found when SS and MBM were gasified, obtaining joint yields of HCN-N, NO-N, tar-N and char-N lower than 5 %, and being NH_3-N (30-67 %) and N_2-N (28-68 %) the majority products. The yields of NH_3-N obtained with GLU (51%), SS (30%), and MBM (67%) under the same gasification operating conditions were significantly different. These differences were attributed to the catalytic effect of the metals present in these residues and points to the need to optimize the operating conditions specifically for each residue. In summary, gasification of SS and MBM may be able to produce around 10% of the NH_3 produced annually in Europe.

Keywords: sewage sludge; meat and bone meal; glutamic acid; gasification; fuel-N; sustainable ammonia.

1. INTRODUCTION

Ammonia (NH_3) is a commodity chemical absolutely necessary for achieving high levels of agriculture production. In fact, NH_3 is one of the most highly produced inorganic chemicals, with a current annual production rate of around 13.5 million tons (NH_3-N) for the European Union in 2018 (Eurostat, 2020) and of around 150 million tons worldwide in 2017 (U.S.G.S., 2018), of which around 85% is used for the production of synthetic fertilizers. On a smaller scale, NH_3 is also utilized for the production of plastics, fibers, explosives, nitric acid, dyes and pharmaceuticals. Apart from these applications, the use

of NH_3 as an energy carrier in order to reduce the carbon dioxide (CO_2) emissions generated in the combustion of fossil fuels and as a hydrogen carrier has been studied in recent years (Service, 2018).

NH_3 is industrially synthesized by the Haber-Bosch process, which is based on a reversible chemical reaction in which the stable atmospheric nitrogen (N_2) reacts with hydrogen (H_2), mainly obtained by natural gas steam reforming, in a catalyst bed at high pressure (100-300 atm) and temperature (400-500 °C) to give NH_3 (N_2 (g) + $3H_2$ (g) $\leftrightarrows$ 2 NH_3 (g) + heat). In terms of energy consumption, industrial NH_3 synthesis is the most energy demanding industrial process for the production of chemicals with an annual global consumption of $2.5 \cdot 10^6$ TJ (Brunning, 2019) and around 3–5% of the total natural gas output (Patil et al., 2015), both due to the production of H_2 by natural gas steam reforming. This process also accounts for roughly 1% of global annual CO_2 emissions, more than any other industrial chemical-making reaction (Boerner, 2019). Consequently, according to experts, there is an urgent need for alternative and more sustainable processes for NH_3 production (Baltrusaitis, 2017). Biomass gasification (Sánchez et al., 2019) and water electrolysis using renewable energy (Wang et al., 2018) have been studied with the aim of obtaining H_2 through a more sustainable process than the steam reforming of natural gas or the partial oxidation of heavy hydrocarbons or coal. There has also been a blossoming interest in the field of electrochemical reduction of N_2 to NH_3 under mild conditions in recent years, due to the potential advantages it could provide in terms of energy requirements, carbon footprint, reactor design and plant simplicity (Cui et al., 2018; Foster et al., 2018).

The Haber-Bosch process also has environmental drawbacks because of the excessive fixation of the stable atmospheric N_2. The huge impact of anthropogenic activities on the earth's nitrogen budget has destabilized the equilibrium state in the biogeochemical

nitrogen (N) cycle and has increased the net content of reactive N-containing compounds in soil, water and the atmosphere (Rockström et al., 2009a; Rockström et al., 2009b). According to Rockström et al. (2009b), humanity has already transgressed three planetary boundaries which, ordered according to their hazard level, are biodiversity loss, imbalance in the N biogeochemical cycle and climate change. These experts estimated that the amount of N_2 removed from the atmosphere for human use should be reduced from 121 million tons (similar value to current consumption) to 35 million tons per year in order to recover a sustainable level in the biogeochemical N-cycle (Rockström et al., 2013; Rockström et al., 2009a; Rockström et al., 2009b). This supports the necessity of developing a sustainable alternative for NH_3 production which should involve not only the use of renewable hydrogen (H) and the reduction of the energy consumption, but also the use of a reactive N source instead of stable atmospheric N_2.

Drawing an analogy with lignocellulosic biomass as a source of renewable carbon (C) for the production of bioenergy and bioproducts, N-rich biological residues, such as sewage sludge, meat and bone meal or manure, could be a possible source of both renewable H and reactive N. The direct application of these residues as agricultural fertilizer is limited by the nature of some of their constituents, such as heavy metals and pathogens, as well as their increasing, centralized and continuous production. Moreover, it is worth noting that the production of these three residues is not negligible. According to European authorities, around 18 $Mt \cdot y^{-1}$ of animal fat and meat industry by-products arise annually in the European Union (EU) from slaughterhouses, dairies and plants producing food for human consumption (Jędrejek et al., 2016). Eurostat database shows a European average production of dry sewage sludge of around 10 $Mt \cdot y^{-1}$ in 2018 (Eurostat, 2019).

As regards a possible process for N recovery in the form of NH_3, it is known that during gasification, the nitrogen contained in the raw material (fuel-N) is mainly released as

NH₃, hydrogen cyanide (HCN), N_2, tar-N and char-N (Leppalahti and Koljonen, 1995). To date, in view of the energetic and synthesis applications of gasification gas, NH₃ and HCN have been considered as pollutants and undesirable compounds because of being precursors of NOx in combustion and poisons for the catalytic post-upgrading of syngas. Therefore, to minimize the formation of such compounds, various aspects have been studied related with the evolution of fuel-N during the gasification of coal, lignocellulosic biomass or combinations of both (Abdoulmoumine et al., 2014; Leppalahti and Koljonen, 1995; Pinto et al., 2007; Zhou et al., 2000) and, to a lesser extent, of N-rich biological residues (Aznar et al., 2009; Paterson et al., 2005; Schweitzer et al., 2018). The mechanism by which fuel-N evolves during gasification depends on the N-functionality (Leppalahti and Koljonen, 1995). In lignocellulosic biomass and other biological raw materials, whose major N-functionality is in the form of proteins, most of the fuel-N is released during the pyrolysis stage (Leppalahti and Koljonen, 1995), and a lesser amount during the char gasification stage (Aznar et al., 2009; Broer and Brown, 2015). NH₃, HCN and tar-N are the main volatile-N species involved in the process. During biomass pyrolysis, the partitioning of fuel-N between volatiles-N and char-N depends on the final temperature and on the char-N functionality, which changes during the pyrolysis process (Wei et al., 2015). Apart from pyrolysis and char gasification reactions, the cracking and reforming of tar-N (Broer and Brown, 2016; Tian et al., 2007) and secondary gas phase reactions (Amure et al., 2003; Broer and Brown, 2015) also influence the final distribution of N among the N-containing products.

The extent of each of the aforementioned reactions may vary significantly with the change in the operating conditions or even by the effect of other raw material constituents, causing variations in the final distribution of the N-containing products obtained from the gasification process. Table 1 shows the fuel-N distribution obtained in previous research

works dealing with gasification of different types of biomass. As can be observed in Table 1, there is great variability in the fuel-N distributions reported in the literature. It is possible to find works in which the major product is either N_2 (Aznar et al., 2009; Broer and Brown, 2016; Zhou et al., 2000) or NH_3 (de Jong et al., 2003; Kurkela and Stahlberg, 1992; Zhou et al., 2000). As regards fuel-N conversion to NH_3-N, values from 10.5% to 63.5% have been obtained in the gasification of Leucaena in a fluidized bed reactor at 950 ºC and 750 ºC, respectively (Zhou et al., 2000), values of around 57% during the gasification of woody biomass at 850 ºC (Jeremias et al., 2014) and of around 19-33% during the gasification of pine (Abdoulmoumine et al., 2014). Table 1 also shows that the conversions of fuel-N to other N-containing products also have very different values ranging from 1.2 to 34% for char-N, from 5.9 to 38% for tar-N and from 0 to 20% for HCN-N. There are only few works in which tar-N compounds have been characterized . In these works, tar-N compounds have been analyzed only qualitatively (Aznar et al., 2009; Gil-Lalaguna et al., 2014) or quantitatively but providing the quantification of only a very small number of tar compounds (Yu et al., 2007).

There is some controversy in the literature about the influence of temperature and the equivalence ratio (ER) on the conversion of fuel-N to NH_3. For example, while some authors claim that as the gasification temperature increases, both the conversion of fuel-N to NH_3-N and the concentration of NH_3 in the gasification gas decrease (Abdoulmoumine et al., 2014; Zhou et al., 2000), some others have observed the opposite trend (Broer and Brown, 2015; Vriesman et al., 2000). The equivalence ratio also has an ambiguous effect on the yield of NH_3, since different studies report a positive effect (Broer and Brown, 2016; Vriesman et al., 2000), a negative effect (Broer et al., 2015) or even a non-significant effect (Abdoulmoumine et al., 2014; Aznar et al., 2009). The effect of other operating conditions on the conversion of fuel-N to NH_3-N seem to be clearer.

For example, both the use of steam as gasifying agent (Cao et al., 2015; Chang et al., 2003) and the use of dolomite as bed material (Cao et al., 2015; Corella et al., 2004; Jeremias et al., 2014) seem to have a positive effect.

Table 1. Summary of fuel-N distribution (%) results in biomass gasification studies reported in the literature.

Raw material	T (ºC)	ER	Gasifying agent	S/C mass ratio	Bed material	char-N (%)	tar-N (%)	HCN-N (%)	NH$_3$-N (%)	N$_2$ (%)
Wood; SS; manure [a]	750-850	0	H$_2$O	2.25	Silica sand; Limestone; Kaolin	-	-	-	35-49	-
Wood [b]	850	0.2	O$_2$+H$_2$O; O$_2$+CO$_2$; O$_2$+ CO$_2$ + H$_2$O	0.2-1.8	Sand; Sand/dolomite mixtures	-	-	-	43-57	-
Cedar Wood [c]	850	0-0.2	O$_2$+H$_2$O	0-2	No bed, updraft gasifier	-	-	<0.2	6-55	-
Miscanthus [d]	700-800	0-0.25	Air	-	Alumina	14-21	-	<0.06	22.4-46.0	-
Cane trash, SS [e]	600-800	-	H$_2$O	-	Zircon sand	-	-	8-20	20-50	-
Switchgrass [f]	750	0-0.40	O$_2$+CO$_2$	-	Silica sand	11-34	21-38	9.8	6-15	11-40
Leucaena; sawdust; bagasse; banagrass [g]	700-900	0.18-0.32	O$_2$+Ar	-	Alumina	1.2-7.7	-	<0.11	10.5-63.5	38.6-88.7
Switchgrass [h]	700-900	0.20-0.40	O$_2$+H$_2$O	1[k]	Silica sand	-	-	2.6-14	32-50	-
Pine [i]	790-1078	0.15-0.35	O$_2$	-	sand	-	-	1.6-2.8	19-33	-
SS [j]	850	0.21-0.30	O$_2$+Ar, Air	-	Ash; SS ash	1.4-8.5	5.9-20.6	0.7-1.6	13.2-28.1	47.4-74.7

[a] (Schweitzer et al., 2018), [b] (Jeremias et al., 2014). [c] (Aljbour and Kawamoto, 2013). [d] (Vriesman et al., 2000). [e] (Tian et al., 2007). [f] (Broer and Brown, 2016). [g] (Zhou et al., 2000). [h] (Broer et al., 2015). [i] (Abdoulmoumine et al., 2014). [j] (Aznar et al., 2009). [k] *Steam to O$_2$ mass ratio*.

Most of the N in lignocellulosic biomass and biological residues is in the form of proteins, peptides and aminoacids, usually referred to as the protein fraction. The protein fraction is the main source of NH$_3$ during gasification. Therefore, the use of a protein or amino acid model compound could be very useful for a first approach to evaluating the effect of

the operating conditions on the chemistry involved in the fuel-N conversion during the gasification of N-rich biological residues, cutting out the effect that the other constituents of the residues may have. Whey and soybean proteins (Hansson et al., 2004; Zhang et al., 2013) and some selected amino acids (Chen et al., 2017; Ren and Zhao, 2012) have previously been used to study the evolution of NOx precursors in the pyrolysis of biomass.

Against this background, the final goal of the research work presented in this paper is to evaluate the sustainable production of NH_3 via gasification of N-rich biological residues as a possible way to deal with two environmental issues: (i) the high demand of resources and the excessive fixation of atmospheric N_2 for the current NH_3 production process and (ii) the management of N-rich biological residues in an environmentally-friendly way. For this purpose, the fuel-N partitioning into NH_3-N, HCN-N, NO-N, char-N and tar-N has been evaluated when gasifying a model amino acid compound (glutamic acid) at different gasification operating conditions (variation of temperature and steam-to-carbon mass ratio). An extensive characterization of the tar product composition was also performed. SS and MBM gasification experiments have been carried out under selected operating conditions with the main aim of assessing the possible production of NH_3 from these residues. We have also compared our results with those found in the literature in order to help to figure out which factors/reactions determine the fuel-N distribution.

2. EXPERIMENTAL

2.1. Characterization of N-rich biological residues: model compound selection

Two N-rich biological wastes, meat and bone meal (MBM) and sewage sludge (SS), were characterized in order to choose a representative N-protein model compound. The nitrogen content in these wastes was 9.9 wt. % and 4.7 wt. %, respectively (analysis with elemental analyzer LECO CHN628 - 628S).

2.1.1. Amino acids analysis (protein hydrolysis)

As mentioned above, most of the fuel-N of these types of waste comes from their protein fraction. The total protein fraction in these three wastes, which includes free amino acids, amino acids in peptides and amino acids in proteins, was measured at the Biological Research Center (CSIC, Spain). Samples were analyzed in duplicate in an ionic chromatograph (Biochrom 30) after hydrolysis. A commercial standard mixture of 17 amino acids was used for calibration: aspartic acid (Asp), threonine (Thr), serine (Ser), glutamic acid (Glu), proline (Pro), glycine (Gly), alanine (Ala), cysteine (Cys), valine (Val), methionine (Met), isoleucine (Ile), leucine (Leu), tyrosine (tyr), phenilaniline (Phe), histidine (His), lysine (Lys) and arginine (Arg).

The total contents of amino acids in MBM and SS (calculated as the sum of the individual concentrations, which are shown in Fig. 1) were 49.8 wt. % and 20.8 wt. %, respectively. The data from the amino acid analyses enabled us to determine the percentage of fuel-N in the form of amino acid-N, that is to say protein-fuel-N, in MBM and SS. These were 78.0 wt.% and 73.1 wt.%, respectively. Glutamic acid (GLU) was the most abundant amino acid in MBM, and the second most abundant in SS. GLU was therefore selected as the N-model compound to be used as raw material in the parametric gasification study.
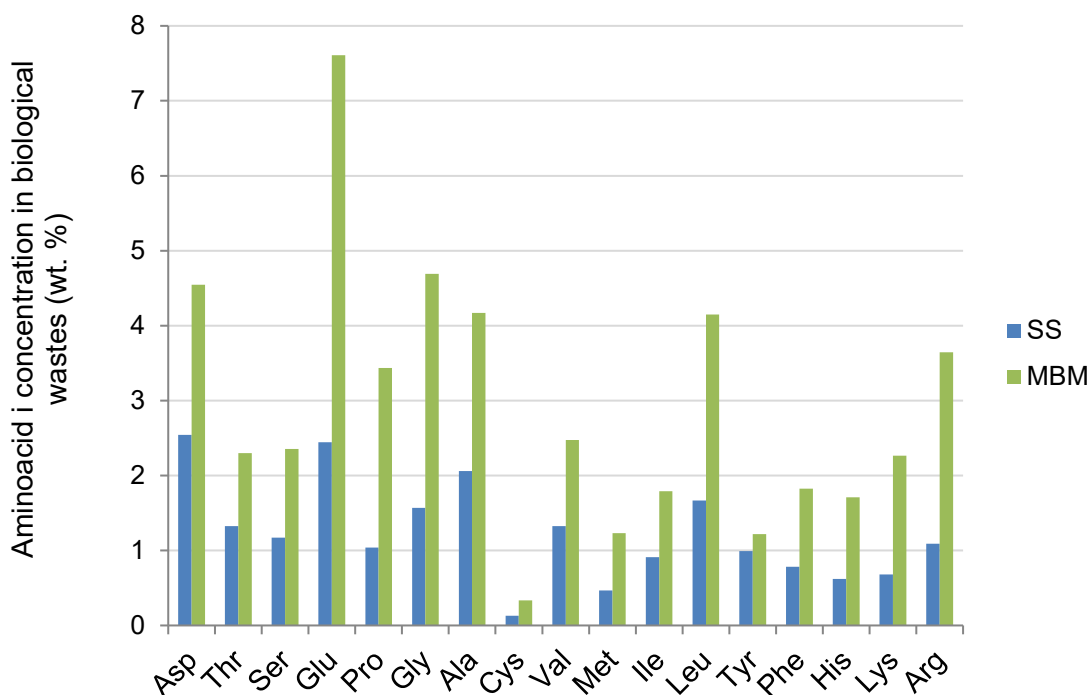
Fig. 1. Content of amino acids in sewage sludge (SS) and meat and bone meal (MBM).

2.2.   Characterization of the raw materials used in the gasification experiments

Gasification experiments were carried out with three different raw materials. Firstly, a parametric gasification study was conducted with GLU in order to evaluate the impact of some operating conditions. Then, SS and MBM were also gasified with the main aim of assessing the potential production of NH_3 from real residues.

Analytical grade L-glutamic acid powder (purity > 99 wt. %) was purchased from Sigma Aldrich, while MBM was supplied by a Spanish animal by-products treatment company and SS came from a Spanish wastewater treatment plant, where SS was anaerobically digested and thermally dried.

The moisture and ash content analyses of GLU, SS and MBM were determined in accordance with EN ISO 18134:2015 and EN ISO 18122:2015, respectively. The elemental analyses were experimentally performed using a LECO CHN 628 Series elemental analyzer. The higher heating values of the three raw materials were determined using a C2000 IKA bomb calorimeter. The results obtained in these analyses are shown in

Table 2. The compositions of the ash in the MBM and SS were determined by inductively coupled plasma optical emission spectroscopy (ICP-OES) and can be seen in Table S1 of the Supplementary information.

Table 2. Composition of the three raw materials (mass fraction %, as received).

	GLU	MBM	SS
Carbon (wt%)	41.0	45.34	27.85
Hydrogen (wt%)[a]	6.0	6.65	4.89
Nitrogen (wt%)	9.5	9.9	4.7
Oxygen (wt%)[b]	43.2	20.14	20.84
Sulfur (wt%)	0.0	0.54	1.41
Ash (wt%)	<0.01	17.40	40.36
Moisture (wt%)	0.3	4.64	7.66
HHV (MJ·kg^{-1})	14.35	20.0	12.4

[a] *The percentage of hydrogen includes hydrogen from moisture.*
[b] *Oxygen was calculated by difference as O(%) = 100 - C(%) - H(%) - N(%) - Ash(%).*

The model amino acid (GLU) was further characterized by thermogravimetric analysis (TGA) and X-ray photoelectron spectroscopy (XPS). Pyrolysis of GLU at 900 ºC under inert atmosphere was carried out in a thermobalance (Netzsch STA 449 F1 Jupiter) and the nitrogen content of the solid product obtained (GLU_PIR900) was determined aiming at following the evolution of the fuel-N remaining in the solid after thermal devolatilization (without taking place any other reaction). In this case, the conversion of fuel-N to char-N at 900 ºC reached 25%, so the rest of the fuel-N (75%) was released in the form of volatiles (gaseous species and tar). On the other hand, the XPS analysis allowed determining the evolution of the N-functionality in GLU after such pyrolysis process. More information about these procedures and results are detailed in the Supplementary Information Section: Thermogravimetric and XPS results of GLU pyrolysis.

2.3. Gasification setup

The gasification runs were conducted in a gasification setup equipped with a laboratory-scale fluidized bed reactor operating at atmospheric pressure. A schematic diagram of the setup is shown in Fig. 2, and more details about the reactor specifications can be found elsewhere (Aznar et al., 2009; Gil-Lalaguna et al., 2014).

Significant operational problems were found when attempting to continuously feed the GLU powder into the reactor with a screw feeder. The material swelled when heated, causing plugging problems in the reactor inlet tube. Cooling of the tube was not enough to prevent this phenomenon. Given these operational problems, the continuous feed of GLU into the gasifier by means of a screw feeder was ruled out. The feeder was replaced by a double valve feeding system placed at the upper part of the reactor. Small tablets of GLU (1.5 cm diameter and 2-3 mm thickness) were prepared with a pressing machine. During the gasification experiments, these tablets were manually fed in pulses of 2.5 g per minute (test duration of 60 min) through the double valve system at the top of the reactor. SS and MBM were fed by the upper double valve system in the same way as GLU in order not to influence the gasification performance. Small tablets of MBM (1.5 cm diameter and 2-3 mm thickness) were also prepared for feeding to the reactor, while SS was fed as received, that is in spherical shape particles (4-5 mm).

The gasifying/fluidizing mixture, composed of air and steam, entered the reactor below the distributor plate and passed through the dolomite bed (~100 g, d_p 350-500 μm). Details about the feeding systems for air and steam are explained elsewhere (Gil-Lalaguna et al., 2014).

After leaving the reactor, particulate matter swept by the gas flow was sequentially removed in a hot cyclone (at a temperature of 600-700 ºC) and in a glass wool hot filter (450 ºC). Tar and water, as well as part of the NH_3 and HCN generated during

gasification, were collected in two condensers arranged in series and cooled at 0.5 ºC with a water-recirculating chiller. After passing through the condensers, the gas was driven through a cotton filter, which retained small aerosols swept up by the gas. The volume of particle- and tar-free gas was continuously measured by a volumetric meter and its composition was analyzed on-line using a micro gas chromatograph (Agilent 3000-A), which determined the volume percentages of H_2, N_2, O_2, CO, CO_2, CH_4, C_2H_4, C_2H_6, C_2H_2 and H_2S. Then, a sample of the gas stream was drawn into a NH_3/HCN absorption trap (absorption bubblers). Sampling and analysis of the NH_3 and HCN collected in the condensers and in the absorption bubblers is explained in greater depth elsewhere (Aznar et al., 2009). At the gas exit, some producer gas was also collected in a Tedlar gas sampling bag for off-line determination of NO by non-dispersive infrared analysis (Advance Optima Infrared Analyzer ModuleUras 14).

Both char and condensed liquid mass yields were determined gravimetrically by weight difference of the corresponding vessels used for their collection. In the case of GLU experiments, the elemental analysis of the solid product was only undertaken on the fraction recovered in the cyclone, since the solid remaining in the bed was essentially pure dolomite, while the solid fraction collected in the hot filter could be polluted with adsorbed tar. In the case of SS and MBM, it was possible to recover some remains of ash/char from the bed to be analyzed. A known mass of methanol was used to wash the condensers and recover the tar. Water content of the mixture was analyzed by Karl Fischer titration, thus obtaining a gravimetric measure of tar by difference.

Tar composition was qualitatively and quantitatively analyzed by gas chromatography with mass spectroscopy and flame ionization detectors (GC-MS/FID). In the Supplementary Information section, Table S2 summarizes the operating parameters for the GC-MS/FID analyses. NIST MS Search Program 2.2 was used for the identification

of the compounds with the MS signal. In addition, the FID signal was calibrated for tar quantification. A commercial standard solution of 16 polycyclic aromatic hydrocarbons (PAH) (PAH Mix 63, 1000 µg·mL^{-1} in toluene, purchased from the Dr. Ehrenstorfer company) and 10 dilutions of it (3-500 µg·mL^{-1} of each compound) were used for calibrating naphthalene and heavier PAH. Moreover, 5 standards of N-containing tar compounds (pyridine, pyrrole, benzonitrile, indole, quinoline) were prepared (80-1500 µg mL^{-1} of each compound) from high-purity chemicals, using a mixture of methanol-dichloromethane (1:1 vol.) as solvent. The FID response factors of the compounds that were identified by GC-MS, but not calibrated as standards, were calculated from the response factor of the most similar standard used, applying to it a correction factor following the methodology based on the Effective Carbon Numbers (ECN) (see the procedure description in the Supplementary Information). ECN theoretical values were calculated following procedures described in the literature (contribution of functional groups to ECN) (Scanlon and Willis, 1985) or directly obtained from the bibliography in the case of some specific compounds (Jorgensen et al., 1990) (see procedure in the Supplementary Information and ECN values in Table S3).
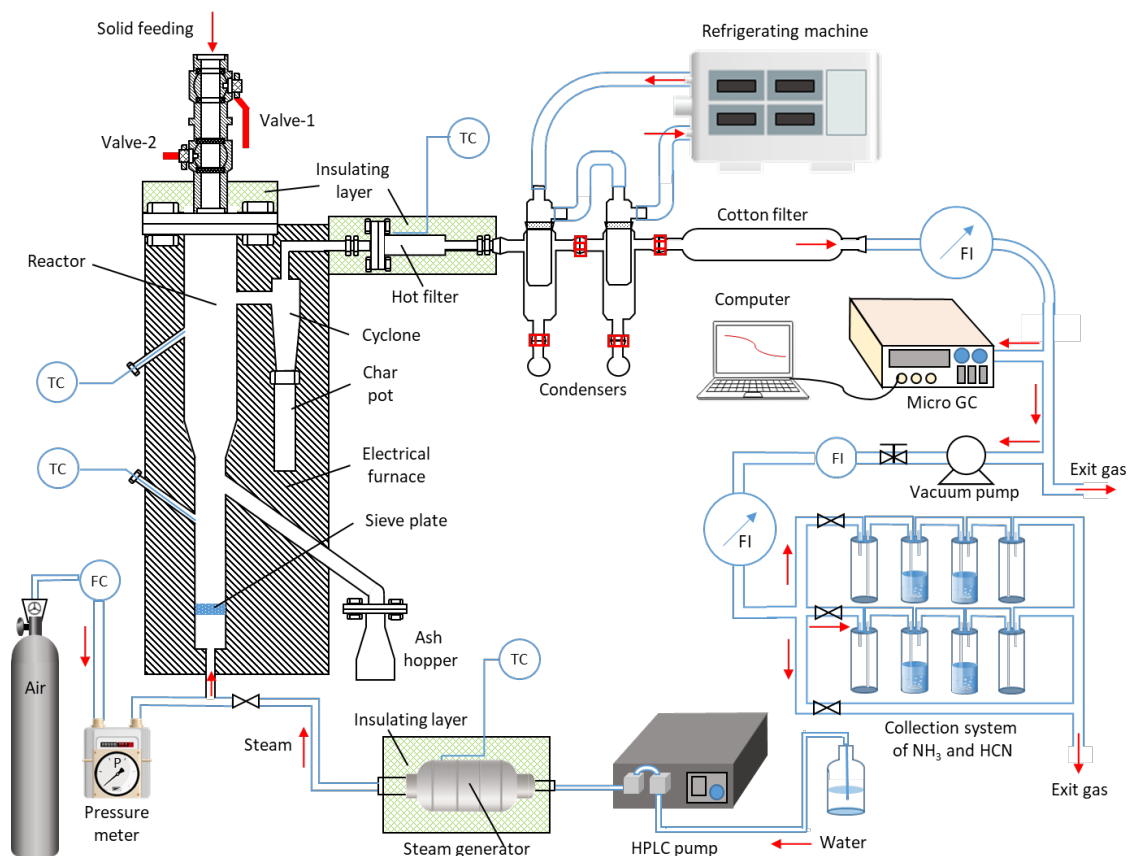
Fig. 2. Schematic diagram of gasification setup (FC: mass flow controller; FI: volumetric flow indicator; TC: temperature controller).

2.4. Operating conditions of the gasification experiments

GLU gasification experiments were planned following a 2^k factorial design aiming at evaluating the impact of the temperature (T) and the steam-to-carbon mass ratio (S/C) on fuel-N partitioning: char-N, tar-N and gas-N in the form of NH_3, HCN and NO. The operating conditions in the GLU, SS and MBM gasification experiments are summarized in Tables 3 and 6.

Most of the works that deal with the chemistry of fuel-N during biomass gasification at atmospheric pressure study the effect of the T and the equivalence ratio *(ER)* as independent variables, although they are dependent in industrial-scale gasification plants (Broer and Brown, 2016; Broer et al., 2015). For this reason, T and *ER* have been

evaluated as dependent variables in the present work. For this purpose, the *ER* required for reaching a specific temperature has been calculated using a non-stoichiometric thermodynamic model. As chemical equilibrium of the gasification reaction is expected to be closely approached at high temperatures, gasification can be modeled with reasonable accuracy using thermodynamic equilibrium models. HSC 9.4.1 software for Excel add-in has been used to model the gasification process. The calculation procedure of the HSC 9.4.1 software is based on (i) minimization of the Gibbs free energy of the system and (ii) atomic mass balance equations. Moreover, (iii) an energy balance has been included in the model by the authors of this work, assuming heat losses of 5%, in order to determine the air input requirement for autothermic conditions. Therefore, for each pair of *T-S/C* values set as operating conditions, the *ER* required for auto-thermal conditions has been calculated (Tables 3 and 6).

Statistical analysis of variance (ANOVA) with a confidence level of 90% was performed to verify the statistical significance of the observed effects and interactions of the two factors. One-way ANOVA coded models have been tested to fit the experimental data. Interpretation of the coded models from one-way ANOVA is explained in depth elsewhere (Fonts et al., 2008).

3. RESULTS

Table 3 summarizes the main operating conditions and the fuel-N distribution obtained in the gasification of GLU. The mass balance in the gasification tests varied from 93 to 100% and the individual atomic balances of C, H, N and O were also close to 100% (89-103%), which points to good experimental procedures. Mass balances can be seen in Table S4 of the Supplementary Information.

Table 3. Operating conditions and experimental results of fuel-N distribution in the gasification of GLU.

	Test 1	Test 2	Test 3	Test 4	Test 5, 6 ,7 [a]
Gasification temperature, ºC	800	900	800	900	850
Steam-to-carbon ratio, g·g⁻¹	0.5	0.5	1	1	0.75
Air feed, g·min⁻¹	5.86	6.36	6.15	6.71	6.26
H_2O feed, g·min⁻¹	0.505	0.505	1.018	1.018	0.761
Equivalence ratio, %	32.4	35.2	34.0	37.2	34.7
Fluidizing velocity, m·s⁻¹ [b]	0.27	0.32	0.31	0.37	0.32
Wet gas velocity in freeboard, m·s⁻¹	0.128	0.147	0.134	0.153	0.138 ± 0.004
Average gas residence time, s [c]	4.9	4.2	4.5	4.0	4.4
Fuel-N distribution (nitrogen yield over fed GLU-N, %)					
NH_3-N	51	35	40	40	45 ± 2
HCN-N	1.0	0.9	1.5	1.4	1.8 ± 0.1
NO-N	0.29	0.20	0.25	0.18	0.21 ± 0.04
Char-N	0.3	0.5	1.4	0.5	0.7 ± 0.1
N-N_2 (by difference)	45	63	55	57	51 ± 2
Tar-N (Total, 1+2)	2.14	0.50	2.04	0.75	1.31 ± 0.03
Tar-N distribution into different families (nitrogen yield over fed GLU-N, %)					
Fuel-N to heterocyclic tar-N (1)	1.77	0.40	1.74	0.62	1.09 ± 0.03
Fuel-N to pyridinic-N (1-a)	1.364	0.265	1.375	0.449	0.816 ± 0.005
Fuel-N to pyrrolic-N (1-b)	0.0311	0.0011	0.0459	0.0017	0.0064 ± 0.0009
Fuel-N to quinolinic-N (1-c)	0.17	0.07	0.11	0.09	0.13 ± 0.02
Fuel-N to indoles(1-d)	0.194	0.065	0.197	0.080	0.140 ± 0.007
Fuel-N to indolizines (1-e)	0.0115	0.0004	0.0108	0.0005	0.0026 ± 0.0001
Fuel-N to aromatic tar-N (2)	0.376	0.097	0.299	0.131	0.215 ± 0.005
Fuel-N to aromatic nitriles (2-f)	0.345	0.081	0.270	0.111	0.191 ± 0.006
Fuel-N to aromatic azides and amines (2-g)	0.031	0.016	0.029	0.020	0.024 ± 0.001

[a] *Results of experiments 5, 6 and 7 are expressed as mean ± standard deviation.*
[b] *The fluidizing velocity only relates to the flow of the gasifying agent (air + steam) passing through the dolomite bed. This velocity was 3-6 times higher than the minimum fluidizing velocity of dolomite (350-500 µm).*
[c] *The residence time of gases and vapors in the reactor was calculated from the reactor volume and the gas flow data (including steam and tar vapors).*

3.1. Fuel-N distribution during glutamic acid gasification

3.1.1. General trends

Fig. 3 shows the partitioning of the fuel-N among the different N-containing products determined experimentally in the GLU gasification experiments.
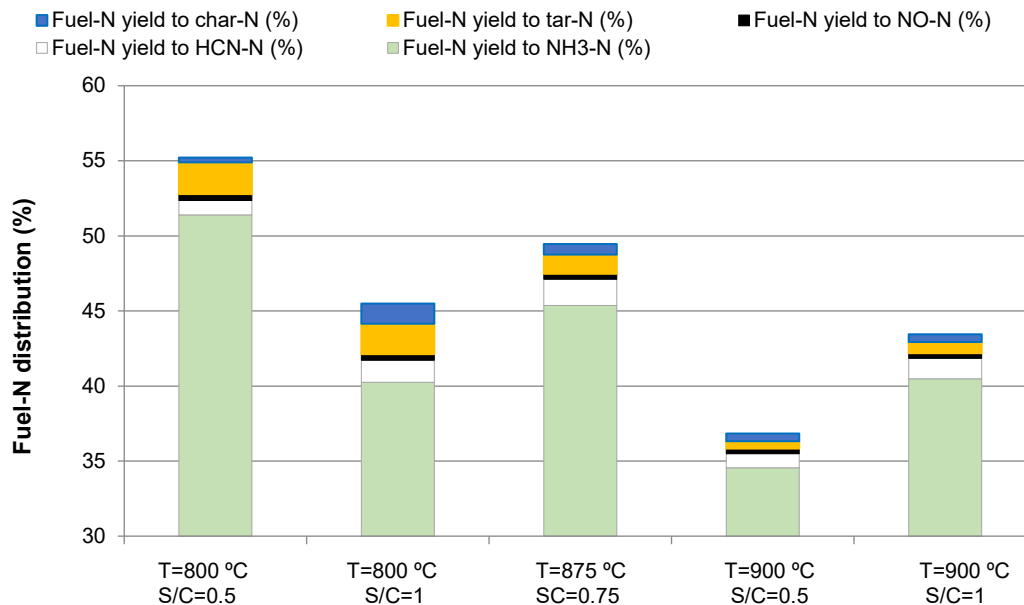
Fig. 3. Fuel-N distribution among the N-containing products determined experimentally in GLU gasification.

The conversion of fuel-N into char-N, tar-N, NO-N, NH_3-N and HCN-N accounted for 38-55% (Fig. 3). NH_3 was the most abundant product among these N-containing compounds determined experimentally, reaching a maximum conversion of fuel-N to NH_3-N of 51 % when the GLU gasification was performed at 800 ºC and with a *S/C* mass ratio of 0.5.

It was attempted to calculate the molecular nitrogen (N_2) generated from the fuel-N as the difference between the mass of N_2 contained in the exit gasification gas (experimentally determined from the micro-GC and the volumetric meter data) and the mass of N_2 introduced into the fluidized bed with the air. However, the results obtained were not consistent due to the high amount of N_2 coming from the gasification agent in comparison with that formed from the raw material. Nevertheless, based on the knowledge of solid fuel-N distribution in biomass gasification processes (Aznar et al., 2009; Broer and Brown, 2016; Zhou et al., 2000) and of the evolution of N-containing gas species according to gas-phase combustion reaction mechanisms under reducing atmosphere

(Glarborg et al., 2018), it is expected that most of the remaining fuel-N that was unable to be properly determined experimentally was in the form of N_2. Hence, the conversion of fuel-N to N_2, obtained by difference, would be between 45 and 62%. Therefore, depending on the operating conditions tested in this gasification work, the main N-containing product could be NH_3 or N_2.

Other N-containing gases such as NO and HCN were produced at small rates, thus obtaining a fuel-N conversion to HCN-N between 0.9 and 1.8%, and < 0.30% in the case of NO-N. In the few works in which the conversion of fuel-N to NO-N or NO_x-N has been determined (Yu et al., 2007; Zhou et al., 2000), the values obtained in all cases were also very low (<0.66 %). HCN-N yields reported in the literature are in a wider range, from 0 to 20% (see Table 1).

Char-N from GLU gasification also accounted for a low percentage of the fuel-N. Comparing the conversion of fuel-N to char-N obtained in these gasification experiments (approximately from 0.3 to 1.4%) and the yield of char-N obtained from the pyrolysis of GLU at 900 ºC (25%) (see Thermogravimetric results in Supplementary Information Section). So, it can be said that fuel-N is released in both devolatilization reactions (pyrolysis) and char gasification reactions.

As commented before, individual species of tar generated in GLU gasification experiments were identified by GC-MS and quantified by the integration of the GC-FID signal. These tar compounds were firstly classified into N-containing tar compounds, which includes two chemical families: (1) heterocyclic tar-N compounds (N atom inside the ring) and (2) aromatic tar-N compounds (N atom outside the ring) and into N-free tar, which mainly refers to PAH (3). The (1) heterocyclic tar-N compounds can, in turn, be classified into five different types: pyridines, pyrroles, quinolones, indoles and indolizines. The (2) aromatic tar-N compounds can be classified into aromatic nitriles,

and aromatic azides and amines. Table S5 in the Supplementary Information Section provides a list of the yields (over fed GLU) of individual species and Table 4 shows the yields of each one of the tar families.

Table 4. Tar yield (g tar·kg^{-1} GLU) distributed into different families.

	Test 1	Test 2	Test 3	Test 4	Test 5, 6 ,7 [a]
Total tar (1+2+3) quantified by GC-FID	15.3	4.5	13.8	6.4	9.6 ± 0.5
N-containing tar (1+2)	13.8	3.4	12.8	5.0	8.5 ± 0.3
Heterocyclic tar-N (1)	11.1	2.7	10.7	4.0	6.9 ± 0.3
Aromatic tar-N (2)	2.74	0.70	2.14	0.95	1.54 ± 0.07
Polycyclic aromatic hydrocarbons (PAH) tar (3)	1.5	1.1	1.0	1.4	1.2 ± 0.1
Fraction of N-containing tar in total tar (wt. %)	90	76	93	78	89 ± 1

As can be observed in Table 4, the total tar yield determined by GC-FID, including PAH-tar and N-containing tar, oscillated between 4.5 and 15.3 g·kg^{-1} over fed GLU. Regardless of the operating conditions, N-containing tar compounds accounted for at least 75 wt.% of the total tar. The fraction of N-containing tar was higher (90-93 wt.%) when operating at the lowest gasification temperature (800 ºC).

Regarding the distribution of fuel-N in the tar-N families, heterocyclic tar-N accounted for more than 80-85% of the total tar-N in most cases. Among heterocyclic tar-N families, pyridinic-N was the most abundant type, accounting for 66-79% of the heterocyclic tar-N.

In the few published works in which tar-N compounds are analyzed by gas chromatography, it was also found that heterocyclic tar compounds accounted for the highest percentage of the chromatographic area (Aznar et al., 2009). Specifically, Yu et al. (2007) found that pyridine was the most abundant compound in the tar mixture.

3.1.2. Effect of the operating conditions on the fuel-N distribution obtained from GLU gasification

Table 5 shows the codified terms and R^2 obtained from the one-way ANOVA of the effect of the temperature and the *S/C* on fuel-N distribution into the different N-containing

products. R^2 is defined as the ratio between the sum of squares explained by the model and the total sum of squares. The lack of fit for all the models provided has been found to be not significant (p-value < 0.1). These models have been used for the building of interaction plots shown in Figures 4 and 5. The model terms shown in Table 5 are usually higher for the temperature than for the *S/C,* which means that the effect of temperature on the fuel-N distribution is greater than the impact of *S/C*.

Table 5. One-way ANOVA model terms for the fuel-N distribution.

Response variable	Independent term	T	S/C	T·S/C	R^2
Fuel-N to char-N (%)	0.68 (± 0.18)	-0.17 (± 0.18) [n.s.]	0.26 (± 0.18)	-0.25 (± 0.18)	0.95
Fuel-N to tar-N (%)	1.36 (± 0.04)	-0.73 (± 0.04)	0.037 (± 0.04)	0.089 (± 0.04)	0.99
Fuel-N to heterocyclic tar-N (%)	1.13 (± 0.04)	-0.62 (± 0.04)	0.048 (± 0.04)	0.061 (± 0.04)	0.99
Fuel-N to aromatic tar-N (%)	0.23 (± 0.005)	-0.11 (± 0.01)	-0.011 (± 0.007)	0.028 (± 0.007)	1.00 [b]
Fuel-N to HCN-N (%)	1.18 (± 0.08)	n.s.	0.24 (± 0.08)	n.s.	0.92 [b]
Fuel-N to NO-N (%)	0.23 (± 0.03)	-0.040 (± 0.035)	n.s.	n.s.	0.60 [a]
Fuel-N to NH₃-N (%)	41.68 (± 2.79)	-4.15 (± 2.79)	-1.31 (± 2.79)	4.27 (± 2.79)	0.95
Fuel-N to N₂ (%)	54.88 (± 2.56)	5.12 (± 2.56)	0.78 (± 2.56)	-4.08 (± 2.56)	0.97 [b]

[n.s.] *not significant term.*
[a] *The overall mean is a better predictor of the response than the current model.*
[b] *Significant curvature.*

Firstly, Fig. 4 shows the interaction plot of the effect of the *T* and the *S/C* mass ratio on the conversion of fuel-N to char-N (a), heterocyclic tar-N (b) and aromatic tar-N (c). It should be noted that both the experimental and the theoretical values resulting from the one-way ANOVA (denoted in the Figure as "Mean ANOVA") have been represented, this showing the good fitting of the models, at least in the high and low levels of the experimental design.
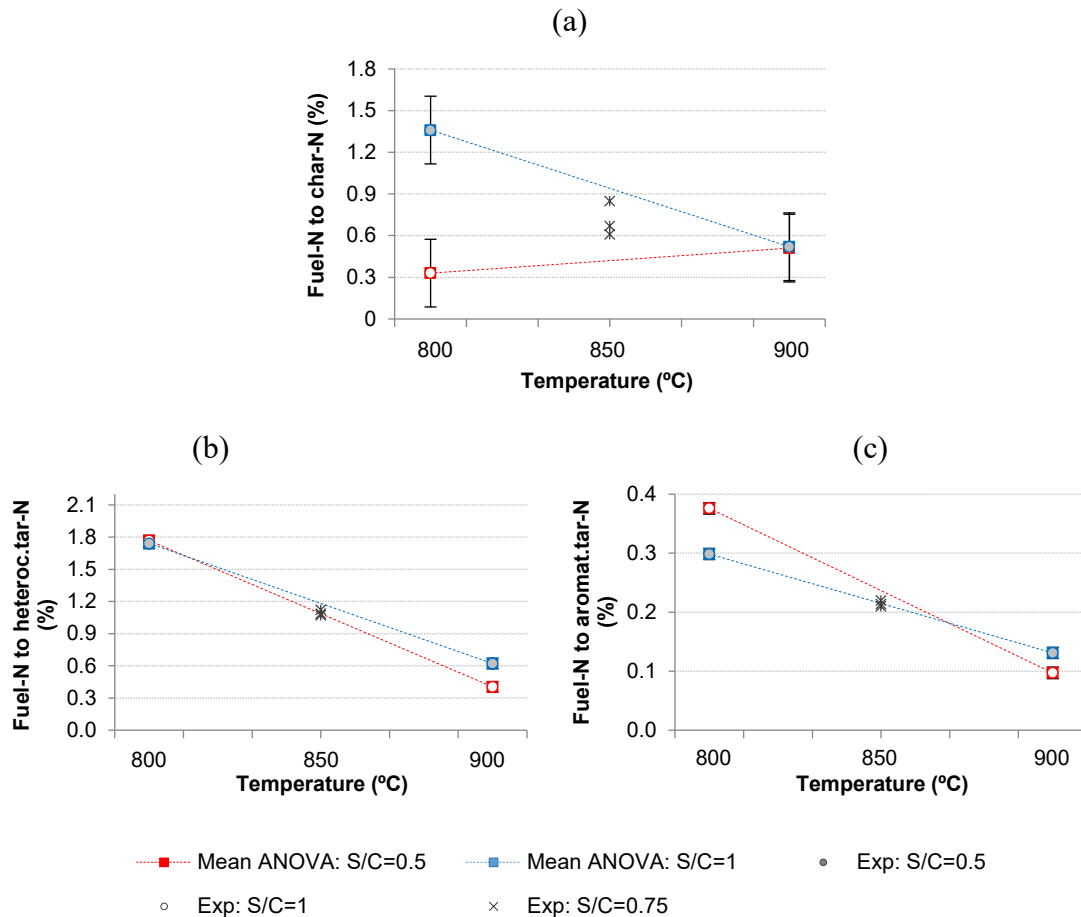
Fig. 4. Effect of temperature and *S/C* mass ratio on the conversion of fuel-N to (a) char-N, (b) heterocyclic tar-N and (c) aromatic tar-N.

In some cases, the effects of the temperature and the *S/C* ratio had a mutual influence in such a way that one factor was only found to be significant at the lowest level of the other. For the lowest temperature, the conversion of fuel-N to char-N decreased as the *S/C* was reduced, indicating a faster kinetic for the remaining solid-N when the gasifying medium contains a higher O_2 concentration.

The conversions of fuel-N to char-N (< 1.5%) obtained in this work were lower than those found by other authors working at similar temperatures but at lower ER and without using steam in the mixture of the gasifying agent (Table 1). For instance, Vriesman et al. (2000) obtained significantly higher conversions of fuel-N to char-N when performing the gasification of miscanthus at lower ER (0-0.25) and slightly lower temperatures (700-

800 ºC) (14% at 700 ºC and ER=0.16). In summary, the release of nitrogen from char seems to be favored by higher temperatures, higher ER and also by the use of steam, which would positively affect the occurrence of devolatilization and char gasification reactions.

On the other hand, the increase in the temperature caused a general decreasing trend in the conversion of fuel-N to heterocyclic tar-N and aromatic tar-N (Fig. 4(b) and 4(c)), this effect in both cases being more marked when using a S/C of 0.5 g·g⁻¹. The interaction of the two factors is significant (as shown in Table 5), and the effect of the S/C on the conversion of fuel-N to both heterocyclic tar-N and aromatic tar-N is different depending on the temperature value. An increase in the S/C ratio caused a rise in the conversion of fuel-N to heterocyclic tar-N and aromatic tar-N at the highest temperature studied (900 ºC), while it provoked a decrease in the aromatic tar-N yield at the lowest temperature studied (800 ºC). The positive effect of the S/C ratio on the yield of tar-N compounds at the highest studied temperature is explained by the behavior of both aforementioned N-containing families, but especially because of the evolution of the subfamily pyridinic tar-N, which is the most abundant N-functionality in tar.

During pyrolysis, the char-N functionalities evolve with the temperature. The N-functionality of the raw material (GLU) and of the char coming from its pyrolysis at 900 ºC (GLU_PIR900) was analyzed by XPS (see XPS results in the Supplementary Information). The deconvolution of the GLU and GLU_PIR900 N 1s spectra (see Figure S1) allowed us to determine that the protein-N functionality (401.5 eV) present in the raw GLU evolved mainly to pyridinic-N (400.5 eV) in the GLU-900. Similar N-functionality results were obtained by Wei et al (2015) when analyzing the evolution of sewage sludge N-functionality during pyrolysis from ambient temperature to 850 ºC. Taking into account this functionality of the char-N at high temperatures (pyridinic-N) and the fact

that the most abundant class in tar is pyridinic-N, it is thought that a higher S/C ratio could promote the formation of this type of compound via char-N gasification reactions (pyridinic char-N (s) + H_2O (g) $\rightarrow$ pyridinic tar-N (g) + other products) (R1).

The fraction of fuel-N that ended up as tar-N compounds in this work (0.5-2.14%) was lower than in other works (see Table 1). The higher values found in the literature (5.9-38%) (Aznar et al., 2009; Broer and Brown, 2016) could be attributed to the fact of using an inert bed (sand) in the reactor (not dolomite like in this work) and/or a lower gasification temperature or equivalence ratio than in this work. Detailed results about the fuel-N distribution among the individual N-containing species in tar is provided in Table S6 (Supplementary Information Section).

Figs. 5(a), 5(b), 5(c) and 5(d) show the effect of the temperature and the S/C mass ratio on the conversion of fuel-N to the gaseous species HCN-N, NO-N, NH_3-N and N_2-N, respectively.
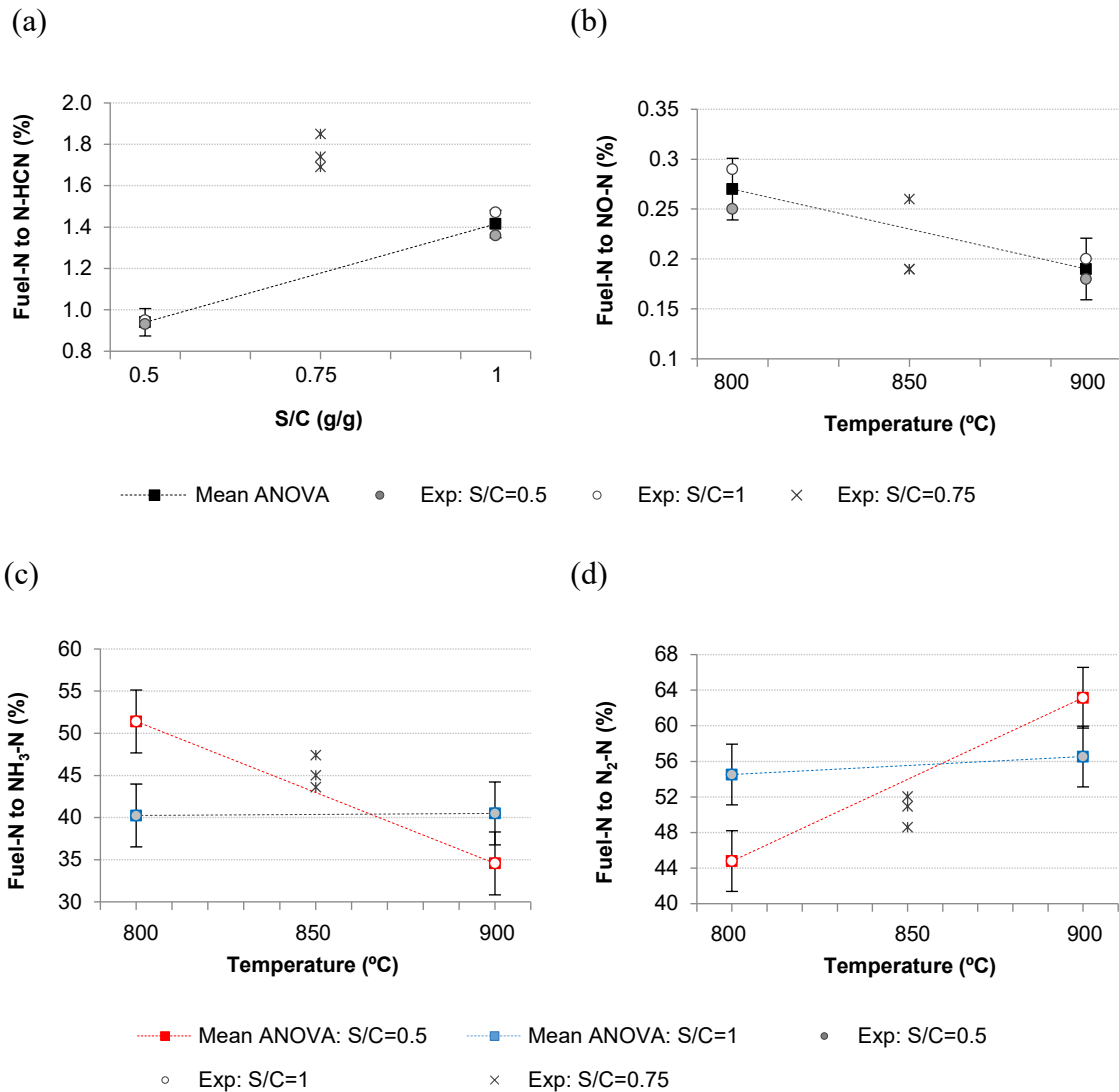
(a)

(b)

(c)

(d)

Fig. 5. Effect of temperature and S/C mass ratio on the conversion of fuel-N to (a) HCN-N, (b) NO-N, (c) NH_3-N and (d) N_2-N.

With respect to the conversion of fuel-N to HCN-N (Fig. 5(a)), the *S/C* ratio was the only factor that showed a significant effect (Table 5), increasing this conversion from 0.9 to 1.4 % when the *S/C* ratio was augmented from 0.5 to 1.0. However, it is worth noting that the conversion of fuel-N to HCN-N presented a curvature within the intervals of temperature and *S/C* studied. Regarding the positive effect of steam presence on the yield to HCN, Paterson et al. (2005) also found that steam addition caused a small rise in the HCN concentration during gasification tests with sewage sludge.

Results reported in the literature regarding the fraction of fuel-N that forms HCN show significant variations. Different studies report conversions significantly higher (9.8-40 %) (Broer and Brown, 2016), lower (0.1 %) (Aljbour and Kawamoto, 2013; Vriesman et al., 2000), and also similar (0.7-1.6 %) (Aznar et al., 2009) to those obtained in this work (0.9-1.8 %). Some authors have observed that HCN is formed from devolatilization reactions of the fuel-N (Broer and Brown, 2015), as well as during the gasification reactions of fuel-N with steam and during the thermal cracking of volatile-N (Tian et al., 2007). However, its formation is also affected by the nitrogen functionality in char (Tian et al., 2014; Vriesman et al., 2000) and by the char reactivity (Tian et al., 2007). On the other hand, HCN is consumed via reactions with H_2 (Cao et al., 2015), H_2O or O_2 (Shimizu et al., 1993). In view of the disparate results found in the literature and the numerous reactions in which HCN takes part, it can be concluded that the conversion of fuel-N to HCN-N is strongly affected by the operating conditions, although some authors have attempted to explain it by an inadequate sampling methodology (Broer et al., 2015). In contrast, the results obtained in this work show that the temperature was the only significant factor in the conversion of fuel-N to NO-N (Fig. 5(b)), showing a slightly negative impact.

Figs. 5(c) and 5(d) show that the effect of the temperature on NH_3-N and N_2-N yields was only significant for the lowest S/C studied (0.5 $g \cdot g^{-1}$). However, while the conversion of fuel-N to NH_3 showed a downward trend with temperature (from 51 % at 800 ºC to 35 % at 900 ºC), the effect of temperature on the fuel-N conversion to N_2 was positive (from 45 % at 800 ºC to 63 % at 900 ºC). Similar effects of the temperature on the conversion of fuel-N to NH_3-N have been obtained by other authors (Abdoulmoumine et al., 2014; Zhou et al., 2000). Likewise, the effect of the S/C ratio was only significant for the lowest temperature studied (800 ºC), decreasing the fuel-N conversion to NH_3 from 51 % to

40 % and increasing the conversion to N_2 when the *S/C* was augmented from 0.5 to 1.0 $g \cdot g^{-1}$. In this regard, Liu and Gibbs (2003) modelled NH_3 emissions obtained in biomass gasification in a fluidized bed and determined that the NH_3 emissions decreased when the moisture of the raw material increased from 10 % to 30 %.

According to the results shown in the literature, during biomass gasification NH_3 takes part as a product or as a reagent in different stages of the reaction. The results obtained by some authors demonstrate its formation during the pyrolysis stage from biomass-N (Aljbour and Kawamoto, 2013; Broer and Brown, 2015; Vriesman et al., 2000). In the specific case of amino acids, Moldoveanu (2010) pointed to several thermal decomposition reactions of amino acids yielding NH_3. One of these reactions is the thermal fragmentation of the amino acid, giving NH_3, CO_2 and alkenes, as shown for GLU in the following reaction ($COOH$-CH_2-CH_2-$CHNH_2$-$COOH$ → NH_3 + $2CO_2$ + CH_3-CH=CH_2; $\Delta H_{298\,K}^{\circ}$ = 166.6 kJ) (R2). NH_3 can also be formed in char-N gasification reactions, as evidenced by results obtained in other studies (Broer and Brown, 2015; Tian et al., 2007). In their biomass gasification model, Liu and Gibbs (2003) proposed some char-N gasification reactions yielding NH_3, which may have occurred during the gasification experiments carried out in this work, (Char-N+CO_2→NH_3+products) (R3) (Char-N+H_2O→NH_3+products) (R4) and (Char-N+H_2→NH_3+products) (R5). The cracking and reforming reactions of tar-N compounds as a source of NH_3 have also been proved by the results found by other authors (Broer and Brown, 2015; Tian et al., 2007). On the other hand, NH_3 also takes part in secondary gas-phase reactions, either as a product (Cao et al., 2015; Shimizu et al., 1993) or as a reagent, although under gasification conditions the gas-phase-reactions leading to the disappearance of NH_3 are predominant. In these secondary gas phase reactions, NH_3 likely disappears as a result of reactions with radicals to form NH_2, which may undergo further decomposition to give N_2 and H_2, giving

as a global reaction (2 NH_3 (g) $\leftrightarrow$ N_2 (g) + 3 H_2 (g); $\Delta H^\circ_{298\ K}$ = 92.38 kJ; ΔG < 0 at T $\geq$

462 K) (R6). Another gas-phase route that could lead to the loss of NH_3 may be its partial

oxidation under reducing conditions (NH_3 (g) + ¾ O_2(g) $\leftrightarrow$ 1/2N_2 (g) + 3/2 H_2O (g);

$\Delta H^\circ_{298\ K}$ = -316.54 kJ; $\Delta S^\circ_{298\ K}$ = 32.7 J·K^{-1}; ΔG < 0 at any temperature) (R7) (Liu and

Gibbs, 2003).

Both NH_3 formation and consuming reactions may be affected by the operating conditions

studied. The final NH_3 yield (measured at the gasifier exit) depends on the overall effect

of the reactions related with the N chemistry (many of them summarized above). In the

case of temperature, it is assumed that if char-N gasification reactions and tar-N cracking

and reforming reactions behave in the same way as those involving non-heteroatom char

and tar, they would be favored by an increase in temperature. At the temperatures studied,

the aforementioned NH_3 consuming reactions (R6 and R7) are completely shifted to the

products side ($K_{p,R6}$(1173 K)=8.1E·10^6 and ($K_{p,R7}$(1173 K)=3.6·10^{15}), although R6 is

more likely to occur to a greater extent due to its lower activation energy. The observed

decrease in the yield of NH_3 with the increase in the *S/C* at 800 ºC could be related with

the higher availability of O_2 (higher *ER*) linked to the highest *S/C*, which could promote

the consuming of NH_3 via R7.

Some of the values found in the literature for the conversion of fuel-N to NH_3-N and N_2-

N (see Table 1) are in consonance with those found in this work (see Tables 3 and 6). As

a general rule, at a low equivalence ratio or at low temperatures the joint yield of HCN-

N, tar-N and char-N are high, while the yield of NH_3 is not usually high (Aznar et al.,

2009; Broer and Brown, 2016; Vriesman et al., 2000). However, if the equivalence ratio

and/or the gasification temperature are sufficiently high, then a significant high yield of

NH_3 can be obtained (Jeremias et al., 2014; Zhou et al., 2000), unless it is reduced in

favor of N_2 production through R6 (Aznar et al., 2009; Zhou et al., 2000). As discussed

previously, the main origin of the N_2 produced from fuel-N is the NH_3 decomposition reaction (R6). The conversions of fuel-N to N_2-N obtained in this work and reported in literature highlight that, under gasification operating conditions, this reaction (R6) does not reach thermodynamic equilibrium, since the obtained experimental concentrations are usually far from the ones calculated for the thermodynamic equilibrium at gasification temperature ranges (for example: $y_{N2} = 0,24997$, $y_{H2} = 0,74992$, $y_{NH3} = 0,011$ at 1100 K and 1 atm). The different extent of this gas phase reaction, in which thermodynamic factors (such as temperature and pressure) and kinetic factors (such as residence time, temperature or catalysis) play a significant role, will be decisive in the final yields of NH_3 and N_2. In fact, the effect that pressure exerts on the thermodynamics of the NH_3 decomposition reaction (R6) was evidenced by the results reported by De Jong et al. (2003) when studied the gasification of miscanthus in a pressurized fluidized bed (0.4-0.7 MPa). In that work, they obtained higher conversions to NH_3-N (94-95%) than those at atmospheric pressure, which shows the shifting of the equilibrium composition to the reagents side as the pressure increases.

Usually the thermodynamic equilibrium composition is not reached during the pyrolysis or gasification of a N-containing raw material, but experimental data in the literature reveal that the decomposition of NH_3 into N_2 tends to occur to a certain extent even at very short gas residence times (around 1 s) (Broer and Brown, 2015). When studying the pyrolysis of switchgrass at temperatures between 650 and 850 ºC, Broer and Brown (2015) reported fuel-N conversions to N_2 between 7 and 35 % when working at short residence times of 1.0-1.2 s. Therefore, the effect of the residence time will be a determining factor in the final fuel-N distribution between NH_3 and N_2.

According to the results obtained in this work, the highest yield of NH_3-N from GLU gasification has been obtained at the lowest temperature studied (800 ºC) and at the lowest

S/C (0.5). Moreover, it can be stated that the enhancing effect of the temperature on the NH_3 decomposition reaction outweighs its positive effect on the reactions involved in its formation (final negative effect of temperature on the net production of NH_3). Lastly, taking into account the general fuel-N distribution obtained, it can be said that, under the operating conditions studied, the disfavoring of the decomposition of NH_3 into N_2 (R6) is of utmost importance in order to achieve a high conversion to NH_3.

3.2. Gasification of N-rich biological residues

The first part of the experimental work in this study used GLU as a model compound for obtaining a first approach to evaluating the influence of the temperature and the *S/C* on the fuel-N distribution during the gasification process. In order to complete the study, some gasification experiments with real N-rich biological residues, such as SS and MBM, were carried out in the same experimental setup under selected operating conditions. Table 6 summarizes the operating conditions and the main results of these experiments. The fuel-N yields to the different N-containing products have been calculated taking the fraction of fuel-N as a basis, but also the specific fraction of protein-fuel-N (see section 2.1.1).

Table 6. Operating conditions and results of the gasification of SS and MBM.

	Tests 8, 9	Test 10	Test 11
Raw material	SS	MBM	MBM
Average gasification temperature (ºC)	800	800	900
Steam-to-carbon (g g^{-1})	0.5	0.5	0.5
Tar yield (g tar·kg^{-1} fed GLU)			
Total tar (1+2+3+4+5)	4.5 ± 0.1	6.4	11.7
Total N-containing tar (1+2)	2.0 ± 0.2	2.7	6.2
Heterocyclic-N tar (1)	0.93 ± 0.05	1.8	2.8
Aromatic-N tar (2)	1.1 ± 0.1	1.0	3.4
PAH tar (3)	2.28± 0.09	3.6	5.1
O-containing tar (without N) (4)	0.09 ± 0.02	0.026	0.21
Heteroatomic-containing tar (without neither N nor O) (5)	0.11 ± 0.03	0.071	0.06
Fraction of N-containing tar in total tar (wt.%)	45 ± 2	42	54
Fuel-N distribution, (% over fuel-N) / (% over protein-fuel-N)			
NH$_3$-N	30/41 ± 1	67/86	34/44
HCN-N	0.451/0.617 ± 0.006	0.823/1.05	0.322/0.413
NO-N	0.61/0.83 ± 0.02	0.49/0.63	0.75/0.96
Tar-N (Total, 1+2)	0.54/0.74 ± 0.05	0.37/0.47	0.79/1.01
Fuel-N to heterocyclic tar-N (1)	0.25/0.43 ± 0.01	0.24/0.31	0.38/0.484
Fuel-N to pyridinic-N (1-a)	0.066/0.090	0.14/0.18	0.17/0.2
Fuel-N to pyrrolic-N (1-b)	0.034/0.047	0.0003/0.0004	0.036/0.046
Fuel-N to quinolinic-N (1-c)	0.075/0.10	0.055/0.070	0.096/0.12
Fuel-N to indoles-N (1-d)	0.077/0.11	0.040/0.051	0.080/0.10
Fuel-N to indolizines-N (1-e)	0	0	0.0081/0.0111
Fuel-N to aromatic tar-N (2)	0.29/0.40	0.13/0.17	0.40/0.52
Fuel-N to aromatic nitriles-N (2-f)	0.27/0.37	0.07/0.09	0.39/0.50
Fuel-N to aromatic azides and amines-N (2-g)	0.02/0.03	0.06/0.08	0.01/0.02
Char-N	0.5/0.7	2.6/3.3	0.36/0.46
N-N$_2$ (by difference)	68/55 ± 1	28/8	64/53

As occurred in the GLU gasification experiments, NH$_3$ and N$_2$ were the majority N-containing products when SS and MBM were gasified. The joint yield of HCN-N, NO-N, char-N and tar-N was similar for the GLU (2.1-3.7% over fuel-N) and for the residues (2.1-4.3% over fuel-N or 2.8-5.5% over protein fuel-N). However, if the fuel-N distribution into these minority products is analyzed in greater depth, significant differences can be found among the raw materials: tar-N accounted for the highest fraction of fuel-N (2.14%) in the case of GLU, NO-N (0.61%) in the case of SS, char-N (2.6%) in the case of MBM at 800 ºC and tar-N (0.79%) in the case of MBM at 900 ºC.

The fuel-N distribution obtained in some of the works shown in Table 1 (Jeremias et al., 2014; Schweitzer et al., 2018; Zhou et al., 2000) is similar to that obtained in this work, in which a low joint yield to char-N, tar-N, HCN-N and NO-N over fuel-N was obtained, while NH_3-N and N_2-N accounted for the highest fuel-N fraction. However, in other works, higher conversions of fuel-N to tar-N (Aznar et al., 2009; Broer and Brown, 2016) and char-N (Broer and Brown, 2016; Vriesman et al., 2000) have been reported. The higher conversions of fuel-N to tar-N obtained in literature works could be related with the low ER, the low temperature, and with the fact that in these works neither dolomite nor steam were used.

Tar compounds generated in the gasification of SS and MBM were analyzed by GC-MS/FID. A greater number of tar compounds were identified in the condensates obtained from the gasification of both residues than in the ones obtained from GLU (see Tables S5, S7 and S8). Apart from the three chemical families appearing in GLU tar: heterocyclic tar-N (1), aromatic tar-N (2) and PAH (3), compounds belonging to two other chemical families (without containing N) were detected: O-containing tar (4) and other heteroatomic containing tar (5). The mass percentage of N-containing tar over total tar was higher in the case of GLU (76-93 wt.% of tar compounds contained N) than for the residues (42-54 wt.% of tar compounds contained N). The PAH-tar fraction in the tar coming from the residues was significantly higher than in the tar coming from GLU. The higher proportion of PAH-tar and the presence of the other two chemical families of compounds is due to the existence of other constituents apart from the N-protein fraction in the residues, which also generate tar during gasification.

Regarding N-containing tar families and subfamilies, heterocyclic tar-N accounted for between 46 % and 65 % of the tar-N in the case of the residues, while it was around 83-85 % when coming from GLU both at 800 and at 900 ºC. The fraction of aromatic tar-N

(over tar-N) generated from the residues (15-30 %) seems to be slightly higher than that generated from GLU under the same operating conditions (6-18 %). As previously mentioned, pyridines were the most abundant compounds among the heterocyclic tar-N obtained in GLU gasification. In the case of MBM, three chemical families were the most abundant: pyridines, nitriles and quinolines. Nitriles stand out from the rest of the families in the SS tar compounds because of their higher proportion. The origin of aromatic nitriles could be the cyclization of fatty nitriles, which are typical compounds generated during the pyrolysis of SS as a consequence of the gas phase reaction between fatty acids and NH_3 released during the pyrolysis stage (Fonts et al., 2017).

The fractions of protein-fuel-N that ended up as NH_3 in the case of SS gasified at 800 ºC (41 %) and MBM gasified at 900 ºC (44 %) were slightly lower than that obtained when GLU was gasified at 800 ºC (51 %). A similar rate of conversion of protein fuel-N into NH_3-N (42 %) was reported by Schweitzer et al. (2018) for the steam gasification of SS (7.1 wt.% N, daf basis) at 800 ºC, using a S/C molar ratio of 1.5 and silica sand as bed material. However, when MBM was gasified at 800 ºC, a significant increase in the yield of NH_3-N over protein-fuel-N (88 %) was observed. The presence of iron-containing minerals, greater in the case of SS than in MBM (see Table S1), can have a catalytic effect promoting the decomposition of NH_3 into N_2 and H_2 (Chen et al., 2011), thus explaining the reduced production of NH_3 from SS in comparison with GLU or MBM. The higher yield of NH_3-N obtained from MBM than from GLU under the same operating conditions (800 ºC and S/C=0.5 g·g^{-1}) could be related to the high content of calcium-containing minerals present in MBM (see Table S1). According to Wei et al. (2018), calcium-containing minerals promote the conversion of protein-N in NH_3 during pyrolysis and could disfavor the decomposition of NH_3 into N_2 and H_2 (Cao et al., 2015). On the other hand, the decrease in the yield of NH_3-N with the temperature observed in the experiments

carried out with MBM matches with the temperature effect observed for the NH_3-N yield in the GLU gasification experiments.

In conclusion, a comparison of these experimental data has shown that although the fuel-N distribution is affected by the raw material used, the general distribution of majority N-containing products (NH_3 and N_2) and minority N-containing products (HCN, NO, tar-N and char-N) remains similar independently of the raw material. In the same way, the decreasing NH_3-N yield with the temperature observed in the GLU gasification experiments was corroborated when MBM was gasified at 800 and 900 ºC.

Taking into account the aforementioned generation of these two N-rich biological residues in the EU and the conversions of fuel-N to NH_3-N obtained, the process proposed in this work could produce around 10% of the NH_3-N produced currently in the EU (13.5 million tons) (Eurostat, 2020) (see the Supplementary Information Section).

4. CONCLUSIONS

A sustainable route for the production of NH_3 has been proposed in this work via autothermal gasification of N-rich biological residues, thereby recycling and converting the reactive nitrogen and the hydrogen contained in these residues into NH_3 and thus enabling their valorization.

The parametric study carried out with a model amino acid compound (glutamic acid: GLU) revealed that the temperature (800-900 ºC) affected the fuel-N distribution more significantly than the steam to carbon (S/C) (0.5-1.0 $g \cdot g^{-1}$) mass ratio. The temperature had a negative effect on the conversion of fuel-N to char-N, heterocyclic tar-N, aromatic tar-N and NH_3-N, while it had a positive effect on the conversion to N_2. Meanwhile, the increase in the S/C had a positive impact on the yield to N-containing tar compounds,

mainly pyridinic tar- N, as well as a negative impact on NH_3 production when operating at 800 ºC.

Under all the operating conditions and raw materials studied (GLU, sewage sludge: SS or meat and bone meal: MBM), a very small fraction of fuel-N was lost in the form of char-N, tar-N, HCN-N and NO-N (joint yields between 2.1-5.2 % of fuel-N). NH_3 and N_2 were the most abundant N-containing products. The MBM gasification experiments confirmed the negative effect of the temperature on the fuel-N conversion into NH_3-N. The different conversion values of fuel-N into NH_3-N obtained from the real residues (30% for SS and 67% for MBM) and that obtained from GLU (51%) were attributed to the effect of the metals present in the residues. The iron-containing minerals of SS would favor the decomposition of NH_3 into N_2, while the calcium-containing minerals of MBM would disfavor this decomposition reaction and favor the conversion of protein-N into NH_3. The optimization of the operating conditions to be used with each raw material, particularly the gasification temperature, is critical to maximize NH_3 production.

Around 10% of the NH_3 produced annually in the EU could be produced by the process proposed in this work, which involves the recycling of the nitrogen and the hydrogen contained in SS and MBM via gasification.

FUNDING

5. REFERENCES

Abdoulmoumine, N., Kulkarni, A., Adhikari, S., 2014. Effects of Temperature and Equivalence Ratio on Pine Syngas Primary Gases and Contaminants in a Bench-Scale Fluidized Bed Gasifier. Ind. Eng. Chem. Res. 53(14), 5767-5777.

Aljbour, S.H., Kawamoto, K., 2013. Bench-scale gasification of cedar wood – Part II: Effect of Operational conditions on contaminant release. Chemosphere 90(4), 1501-1507.

Amure, O., Hanson, S., Cloke, M., Patrick, J.W., 2003. The formation of ammonia in air-blown gasification: does char-derived NO act as a precursor? Fuel 82(15-17), 2139-2143.

Aznar, M., San Anselmo, M., Manya, J.J., Benita Murillo, M., 2009. Experimental Study Examining the Evolution of Nitrogen Compounds during the Gasification of Dried Sewage Sludge. Energy Fuels 23, 3236-3245.

Baltrusaitis, J., 2017. Sustainable Ammonia Production. ACS Sust. Chem. Eng. 5(11), 9527-9527.

Boerner, L.K., 2019. Industrial ammonia production emits more CO_2 than any other chemical-making reaction. Chemists want to change that. Cehemical and Engineering News 97(24), 18-22.

Broer, K.M., Brown, R.C., 2015. The role of char and tar in determining the gas-phase partitioning of nitrogen during biomass gasification. Applied Energy 158, 474-483.

Broer, K.M., Brown, R.C., 2016. Effect of Equivalence Ratio on Partitioning of Nitrogen during Biomass Gasification. Energy Fuels 30(1), 407-413.

Broer, K.M., Woolcock, P.J., Johnston, P.A., Brown, R.C., 2015. Steam/oxygen gasification system for the production of clean syngas from switchgrass. Fuel 140, 282-292.

Brunning, A., 2019. Periodic Graphics: Environmental Impact of Industrial Reactions. Chem. Eng. News 97(24), 23.

Cao, J.P., Huang, X., Zhao, X.Y., Wei, X.Y., Takarada, T., 2015. Nitrogen transformation during gasification of livestock compost over transition metal and Ca-based catalysts. Fuel 140, 477-483.

Corella, J., Toledo, J.M., Padilla, R., 2004. Olivine or dolomite as in-bed additive in biomass gasification with air in a fluidized bed: Which is better? Energy Fuels 18(3), 713-720.

Cui, X., Tang, C., Zhang, Q., 2018. A Review of Electrocatalytic Reduction of Dinitrogen to Ammonia under Ambient Conditions. Advanced Energy Materials 8(22), 1800369.

Chang, L., Xie, Z., Xie, K.-C., Pratt, K.C., Hayashi, J.-i., Chiba, T., Li, C.-Z., 2003. Formation of NOx precursors during the pyrolysis of coal and biomass. Part VI. Effects of gas atmosphere on the formation of NH3 and HCN. Fuel 82(10), 1159-1166.

Chen, H., Namioka, T., Yoshikawa, K., 2011. Characteristics of tar, NOx precursors and their absorption performance with different scrubbing solvents during the pyrolysis of sewage sludge. Applied Energy 88(12), 5032-5041.

Chen, H., Si, Y., Chen, Y., Yang, H., Chen, D., Chen, W., 2017. NOx precursors from biomass pyrolysis: Distribution of amino acids in biomass and Tar-N during devolatilization using model compounds. Fuel 187, 367-375.

de Jong, W., Ünal, Ö., Andries, J., Hein, K.R.G., Spliethoff, H., 2003. Thermochemical conversion of brown coal and biomass in a pressurised fluidised bed gasifier with hot gas filtration using ceramic channel filters: measurements and gasifier modelling. Applied Energy 74(3), 425-437.

Eurostat, 2019. Sewage sludge production and disposal. https://ec.europa.eu/eurostat/web/environment/water. (Accessed 31/01/2020).

Eurostat, 2020. Production of NH3-N in EU (28 countries) in 2018. https://ec.europa.eu/eurostat/web/prodcom/data/database?p_p_id=NavTreeportletprod_WAR_NavTreeportletprod_INSTANCE_iSpjsGQt409q&p_p_lifecycle=0&p_p_state=normal&p_p_mode=view&p_p_col_id=column-2&p_p_col_count=1. (Accessed 14/04/2020).

Fonts, I., Juan, A., Gea, G., Murillo, M.B., Sanchez, J.L., 2008. Sewage sludge pyrolysis in fluidized bed, 1: Influence of operational conditions on the product distribution. Ind. Eng. Chem. Res. 47(15), 5376-5385.

Fonts, I., Navarro-Puyuelo, A., Ruiz-Gomez, N., Atienza-Martinez, M., Wisniewsky, A., Gea, G., 2017. Assessment of the Production of Value-Added Chemical Compounds from Sewage Sludge Pyrolysis Liquids. Energy Technol. 5(1), 151-171.

Foster, S.L., Bakovic, S.I.P., Duda, R.D., Maheshwari, S., Milton, R.D., Minteer, S.D., Janik, M.J., Renner, J.N., Greenlee, L.F., 2018. Catalysts for nitrogen reduction to ammonia. Nature Catalysis 1(7), 490-500.

Gil-Lalaguna, N., Sánchez, J.L., Murillo, M.B., Rodríguez, E., Gea, G., 2014. Air-steam gasification of sewage sludge in a fluidized bed. Influence of some operating conditions. Chem. Eng. J. 248, 373-382.

Glarborg, P., Miller, J.A., Ruscic, B., Klippenstein, S.J., 2018. Modeling nitrogen chemistry in combustion. Prog. Energy Combust. Sci. 67, 31-68.

Hansson, K.-M., Samuelsson, J., Tullin, C., Åmand, L.-E., 2004. Formation of HNCO, HCN, and NH3 from the pyrolysis of bark and nitrogen-containing model compounds. Combust. Flame 137(3), 265-277.

Jędrejek, D., Levic, J., Wallace, J., Oleszek, W., 2016. Animal by-products for feed: characteristics, European regulatory framework, and potential impacts on human and animal health and the environment. Journal of Animal and Feed Sciences 25(3), 189-202.

Jeremias, M., Pohorely, M., Bode, P., Skoblia, S., Beno, Z., Svoboda, K., 2014. Ammonia yield from gasification of biomass and coal in fluidized bed reactor. Fuel 117, 917-925.

Jorgensen, A.D., Picel, K.C., Stamoudis, V.C., 1990. Prediction of gas chromatography flame ionization detector response factors from molecular structures. Anal. Chem. 62(7), 683-689.

Kurkela, E., Stahlberg, P., 1992. Air Gasification of Peat, Wood and Brown Coal in a Pressurized Fluidized Bed Reactor. 2. Formation of Nitrogen-Compounds. Fuel Process. Technol. 31(1), 23-32.

Leppalahti, J., Koljonen, T., 1995. Nitrogen Evolution from Coal, Peat and Wood during Gasification - Literature Review. Fuel Process. Technol. 43(1), 1-45.

Liu, H., Gibbs, B.M., 2003. Modeling NH_3 and HCN emissions from biomass circulating fluidized bed gasifiers. Fuel 82(13), 1591-1604.

Moldoveanu, S.C., 2010. Pyrolysis of Organic Molecules with Applications to Health and Environmental Issues, in: Moldoveanu, S.C. (Ed.) Techniques and Instrumentation in Analytical Chemistry. Elsevier, p. 724.

Paterson, N., Zhuo, Y., Dugwell, D., Kandiyoti, R., 2005. Formation of Hydrogen Cyanide and Ammonia during the Gasification of Sewage Sludge and Bituminous Coal. Energy Fuels 19(3), 1016-1022.

Patil, B.S., Wang, Q., Hessel, V., Lang, J., 2015. Plasma N2-fixation: 1900–2014. Catal. Today 256, 49-66.

Pinto, F., Lopes, H., Andre, R.N., Gulyurtlu, I., Cabrita, I., 2007. Effect of catalysts in the quality of syngas and by-products obtained by co-gasification of coal and wastes. 1. Tars and nitrogen compounds abatement. Fuel 86(14), 2052-2063.

Ren, Q., Zhao, C., 2012. NOx and N2O precursors from biomass pyrolysis: Nitrogen transformation from amino acid. Environ. Sci. Technol. 46(7), 4236-4240.

Rockström, J., Sachs, J.D., Öhman, M.C., Schmidt-Traub, G., 2013. Sustainable Development and Planetary Boundaries, Background paper for the High-Level Panel of Eminent Persons on the Post-2015 Development Agenda, United Nations. p. 45.

Rockström, J., Steffen, W., Noone, K., Persson, Å., Chapin, F.S., III, Lambin, E., Lenton, T.M., Scheffer, M., Folke, C., Schellnhuber, H.J., Nykvist, B., de Wit, C.A., Hughes, T., van der Leeuw, S., Rodhe, H., Sörlin, S., Snyder, P.K., Costanza, R., Svedin, U., Falkenmark, M., Karlberg, L., Corell, R.W., Fabry, V.J., Hansen, J., Walker, B., Liverman, D., Richardson, K., Crutzen, P., Foley, J., 2009a. Planetary Boundaries: Exploring the Safe Operating Space for Humanity. Ecol. Soc. 14(2).

Rockström, J., Steffen, W., Noone, K., Persson, A., Chapin, F.S., III, Lambin, E.F., Lenton, T.M., Scheffer, M., Folke, C., Schellnhuber, H.J., Nykvist, B., de Wit, C.A., Hughes, T., van der Leeuw, S., Rodhe, H., Sorlin, S., Snyder, P.K., Costanza, R., Svedin, U., Falkenmark, M., Karlberg, L., Corell, R.W., Fabry, V.J., Hansen, J., Walker, B., Liverman, D., Richardson, K., Crutzen, P., Foley, J.A., 2009b. A safe operating space for humanity. Nature 461(7263), 472-475.

Sánchez, A., Martín, M., Vega, P., 2019. Biomass Based Sustainable Ammonia Production: Digestion vs Gasification. ACS Sust. Chem. Eng. 7(11), 9995-10007.

Scanlon, J.T., Willis, D.E., 1985. Calculation of Flame Ionization Detector Relative Response Factors Using the Effective Carbon Number Concept. J. Chromatogr. Sci. 23(8), 333-340.

Schweitzer, D., Gredinger, A., Schmid, M., Waizmann, G., Beirow, M., Spörl, R., Scheffknecht, G., 2018. Steam gasification of wood pellets, sewage sludge and manure: Gasification performance and concentration of impurities. Biomass Bioenergy 111, 308-319.

Service, R.F., 2018. Liquid sunshine. Science 361(6398), 120-123.

Shimizu, T., Ishizu, K., Kobayashi, S., Kimura, S., Shimizu, T., Inagaki, M., 1993. Hydrolysis and oxidation of hydrogen cyanide over limestone under fluidized bed combustion conditions. Energy Fuels 7(5), 645-647.

Tian, F.-J., Yu, J., McKenzie, L.J., Hayashi, J.-i., Li, C.-Z., 2007. Conversion of fuel-N into HCN and NH_3 during the pyrolysis and gasification in steam: A comparative study of coal and biomass. Energy Fuels 21(2), 517-521.

Tian, K., Liu, W.-J., Qian, T.-T., Jiang, H., Yu, H.-Q., 2014. Investigation on the Evolution of N-Containing Organic Compounds during Pyrolysis of Sewage Sludge. Environ. Sci. Technol. 48(18), 10888-10896.

U.S.G.S., 2018. U.S. Geological Survey, 2018, Mineral commodity summaries 2018: U.S. Geological Survey, pp. 117, http://doi.org/10.3133/70194932. , in: U.S. Department of the Interior, U.S.G.S. (Ed.). p. 117.

Vriesman, P., Heginuz, E., Sjostrom, K., 2000. Biomass gasification in a laboratory-scale AFBG: influence of the location of the feeding point on the fuel-N conversion. Fuel 79(11), 1371-1378.

Wang, L., Xia, M., Wang, H., Huang, K., Qian, C., Maravelias, C.T., Ozin, G.A., 2018. Greening Ammonia toward the Solar Ammonia Refinery. Joule 2(6), 1055-1074.

Wei, L., Liu, M., Liang, F., Yang, T., Wen, L., 2018. Effects of CaO on nitrogen transformation during pyrolysis of soybean protein. Energy Sources, Part A: Recovery, Utilization, and Environmental Effects 40(22), 2641-2647.

Wei, L., Wen, L., Yang, T., Zhang, N., 2015. Nitrogen Transformation during Sewage Sludge Pyrolysis. Energy Fuels 29(8), 5088-5094.

Yu, Q.Z., Brage, C., Chen, G.X., Sjostrom, K., 2007. The fate of fuel-nitrogen during gasification of biomass in a pressurised fluidised bed gasifier. Fuel 86(4), 611-618.

Zhang, J., Tian, Y., Cui, Y., Zuo, W., Tan, T., 2013. Key intermediates in nitrogen transformation during microwave pyrolysis of sewage sludge: A protein model compound study. Bioresour. Technol. 132(Supplement C), 57-63.

Zhou, J., Masutani, S.M., Ishimura, D.M., Turn, S.Q., Kinoshita, C.M., 2000. Release of Fuel-Bound Nitrogen during Biomass Gasification. Ind. Eng. Chem. Res. 39(3), 626-634.